Chapter 7

Implementing Quantum Finite Automata

Our active learning method explained in Chapter 6 can be used, for example, to construct a noise-free model from a photon optical experiment that manipulates laser through linear optical elements. In this chapter we consider, by way of experiment, the converse: implementing an MO-1QFA by linear optical elements.

Some proof-of-principle experiments have been performed to prove the quantum benefits of QFA [116, 75]. In these experiments, a prevailing approach involves reading the entire input string before initiating the experimental process. This approach presumes prior knowledge of the string's length, compelling the allocation of additional memory resources to store this length information and necessitate the placement of unitary operators in the form of half-wave plates (HWPs) *after* the entire input has been read. Importantly, this approach deviates from the conventional principles of automata theory, where the automaton should inherently operate without prior knowledge of the input size. This raises questions about the adherence of such methodologies to the foundational principles of automata theory and the extent to which they truly harness the potential of quantum computation.

In this chapter, we devise a novel solution that addresses this challenge. We use a specialized apparatus to read the input string. Remarkably, with each occurrence of a symbol being read, this device automatically triggers the precise rotation of the corresponding HWP. This innovative strategy ensures that we do not explicitly obtain the length information of the input string. Instead, the length information is implicitly encoded within the rotations of the HWPs. This methodology effectively eliminates the need for additional memory to store the input length, thus aligning more faithfully with the principles of automata theory. To the best of our knowledge, this work presents the first successful implementation of quantum finite automata that operates without prior knowledge of the input string's length.

7.1 Implementing a regular language

In this section, we give the details on how to implement a simple MO-1QFA using linear optics. As a proof of concept, we first concentrate on an automaton on a single-letter alphabet that recognizes with unbounded probability error the regular language $\{a\}^*$.

Let $\Sigma = \{a\}$ an alphabet consisting of a single letter and consider the MO-1QFA M with two states $Q = \{q_1, q_2\}$ of which q_1 is both initial and the unique accepting state. The evolution matrix for a is given by the unitary operator

$$\boldsymbol{U}_\theta = \begin{pmatrix} cos\theta & -sin\theta \\ sin\theta & cos\theta \end{pmatrix}$$

where θ is an angle between 0 and 90 degree, the latter not included. When reading the string a^k for some $k \geq 0$ from the initial state $|q_1\rangle$, the state of the automaton will be

$$|\psi_k\rangle = cos(k\theta)|q_1\rangle + sin(k\theta)|q_2\rangle.$$

and the string a^k is thus accepted with probability $cos^2 k\theta$. Since for any k, all these probabilities are strictly positive, the automaton accepts with unbounded probability error the set $\{a\}^*$.

Note that if we let $\boldsymbol{U}_{\alpha\theta}$ be a rotation with an irrational α [104], since $\boldsymbol{U}_{\alpha\theta}$ is dense on the unit circle, for any given two different cutpoints λ_1 and λ_2, there exists a k such that the accepting probability of accepting a^k lies between λ_1 and λ_2. As a result, the languages L_{λ_1} and L_{λ_2} accepting with bounded probability error at least λ_1 and λ_2, respectively, are different if $\lambda_1 \neq \lambda_2$. In particular, we will have $L_{\lambda_2} \subset L_{\lambda_1}$.

7.1.1 The implementation

We now present our experimental implementation of the above MO-1QFA in linear optics. As shown in Figure 7.1, the experimental setup consists of four parts: single-photon source, state preparation, implementation, and measurement. The experimental setup is designed to realize a MO-1QFA with the capability to discern the occurrences of the symbol a within a given string. The photon's polarization state serves as the carrier of information, and its evolution is realized by two Half-Wave Plates (HWPs). Measurement is executed through a conjunction of an HWP and a Polarizing Beam Splitter (PBS).

More in detail, the single photon source generates heralded single photons, each with a central wavelength of 404nm, achieved through the utilization of a UV laser to stimulate a type-I beta barium borate (BBO) crystal. One photon serves as a trigger and the other as a

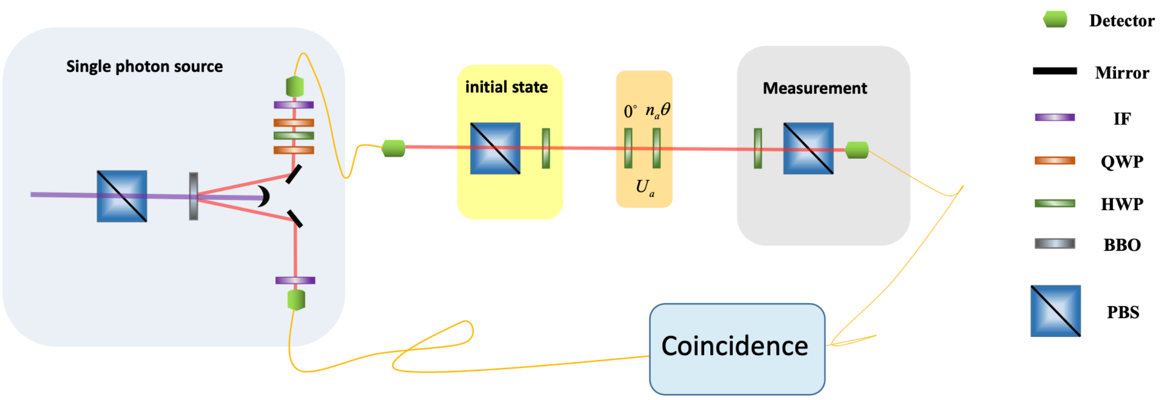

Fig. 7.1 First Experimental Setup of an Optical MO-1QFA.

signal photon. Because of the disturbance of the single-mode fiber to polarization, the signal photon needs to pass through the sandwich structure (QWP-HWP-QWP) to eliminate this influence.

Following this, a PBS and a HWP are used to prepare the photon in the required state. The first photon is encoded in polarization degree of freedom. Through the combination of a PBS and an HWP set at $0°$, the photon is set to the state $|H\rangle$ (where H denotes horizontal polarization and corresponds to the automaton state q_1). The second photon is then directed through the optical circuit, facilitated by the coincidence detection process at the detectors.

Subsequently, the photon undergoes a series of unitary operations, which encompass $\boldsymbol{U}_\theta$, and a final measurement (M). The unitary operator $\boldsymbol{U}_\theta$ is realized through the use of two sequential HWPs.

The measurement setup consists of a HWP in conjunction with a PBS. When the HWP sets at $0°$, we could measure the state $|H\rangle$. Subsequently, with an adjustment to $45°$, the polarization shifts from H to V and vice versa, enabling the assessment of the state $|V\rangle$, where V denotes vertical polarization (representing the automaton state q_2). This sequential measurement allows for the computation of the probability associated with the state $|H\rangle$.

Notably, we exclusively use the polarization property of this photon to represent two states within this MO-1QFA. Meanwhile, the second photon is dedicated to coincidental measurement, ensuring the presence of the primary photon within the optical path.

The application of U_a is executed through the arrangement of two HWPs in tandem. Each detection of an a initiates a clockwise rotation of the second HWP of $\boldsymbol{U}_\theta$ by a precise $7°$, leading to the unitary operator with $theta = 14°$, that is $\boldsymbol{U}_{14°} = \begin{pmatrix} \cos 14° & -\sin 14° \\ \sin 14° & \cos 14° \end{pmatrix}$. As the occurrences of a accumulate to n, this iterative process advances the operator

Table 7.1 Observed probabilities in time for a few strings.

	0.5s	1s	1.5s	2s	2.5s	3s	4s
ε	0.9968	0.9964	0.9968	0.9965	0.9966	0.9964	0.9966
a	0.9408	0.9395	0.9404	0.9410	0.9409	0.9400	0.9401
aa	0.7825	0.7833	0.7780	0.7811	0.7834	0.7819	0.7816
aaa	0.5546	0.5505	0.5591	0.5547	0.5549	0.5539	0.5545
aaaa	0.3214	0.3173	0.3194	0.3165	0.3159	0.3168	0.3166
aaaaa	0.1158	0.1196	0.1182	0.1170	0.1212	0.1202	0.1196
aaaaaa	0.0133	0.0125	0.0122	0.0125	0.0129	0.0124	0.0125
aaaaaaa	0.0197	0.0210	0.0214	0.0199	0.0205	0.0204	0.0209
aaaaaaaa	0.1453	0.1459	0.1439	0.1426	0.1413	0.1418	0.1418
aaaaaaaaa	0.3412	0.3406	0.3454	0.3430	0.3452	0.3439	0.3447

$\begin{pmatrix} \cos n14^\circ & -\sin n14^\circ \\ \sin n14^\circ & \cos n14^\circ \end{pmatrix}$. The measurement procedure is as follows. Initially, the HWP is positioned at 0° to measure the state $|H\rangle$, followed by an adjustment to 45° to measure the state $|V\rangle$. This sequence enables us to ascertain the probability of the system being in state $|H\rangle$.

7.1.2 Running a few experiments

We have run a few experiments to check the goodness of our implementation. The results of this experiment are presented in Table 7.1, which provides insights into the MO-1QFA's performance in identifying varying quantities of a symbols across different time intervals. Table 7.1 presents the probabilities of the MO-1QFA accurately recognizing the number of a in a string, within time intervals ranging from 0.5 to 4 seconds. The rows of the table correspond to different string configurations, such as the empty string, a single occurrence of a, or some repeated sequences of a.

Upon analyzing the results, several observations can be made. Notably, the probabilities associated with each string configuration tend to stabilize as the time interval increases. This suggests that the accuracy of our optical implementation of a MO-1QFA's accuracy improves with longer observation periods.

This experiment represents an idealized scenario where, in theory, we employ irrational numbers for our operations. However, practical limitations prevent us from achieving such precision. For instance, in our experiment, we use a 7° rotation. Under ideal conditions, the angle should hold indefinitely, but in reality, it inevitably leads to a point of repetition, as demonstrated by the occurrence of repeating digits after processing 90 occurrences of the symbol a. Even if we were to use irrational numbers for our angular measurements, the readout probabilities we obtain are still finite rational numbers (they are calculated using the frequency of certain observations). This inherent limitation stems from the current state of technology. Thus, while we may aspire to implement irrational angles, our existing techniques only allow us to confirm the presence of a specific pattern within a given string.

7.2 Implementing a non-regular language

In the classical setting, nondeterministic finite automata (PFAs with cutpoint 0) are limited to defining only regular languages. Next, we proceed by implementing in linear optics a more complex MO-1QFA, recognizing strings on a two-letter alphabet $\Sigma = \{a, b\}$. In particular, we will consider the automaton from Example 17 in the previous Chapter that we have seen accepting with unbounded probability the non-regular language $L = \{x \in \Sigma^* \mid |x|_a \neq |x|_b\}$.

7.2.1 The implementation

The second experimental setup of an optical MO-1QFA is designed to determine whether it reads an equal number of a's and b's. The structure presented in Figure 7.2 is analog to that we used previously.

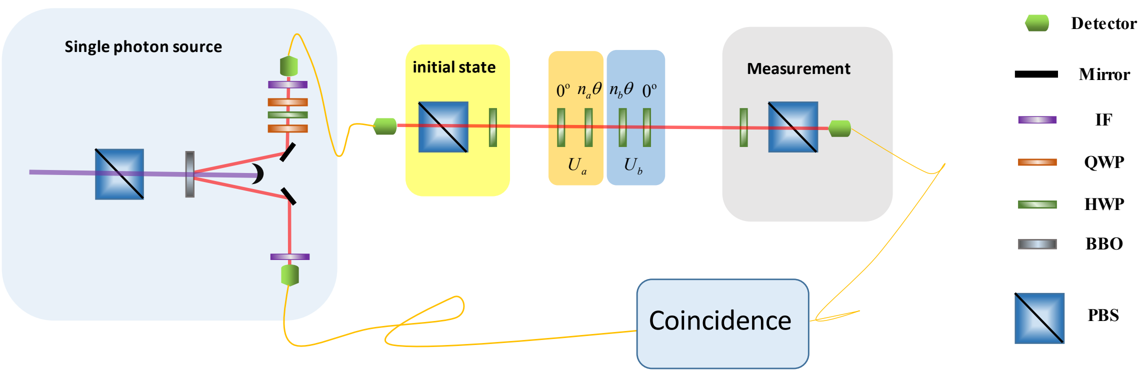

Fig. 7.2 Second Experimental Setup of an Optical MO-1QFA.

Similar to the first experimental setup, a photon pair with a central wavelength at 404 nm is generated by pumping a type-I BBO crystal with a UV laser. The information of the photon is encoded within its polarization state. We utilize only the horizontal and vertical polarization degrees, characterizing the two distinct states of the automaton. The other photon plays a crucial role in coincidence measurement, ensuring the presence of the first photon in the optical path. The evolution is governed by a series of unitary operators including $\boldsymbol{U}_a$ and $\boldsymbol{U}_b$, facilitated by the presence of two HWPs. Ultimately, the measurement process is enacted through a combination of an HWP and a PBS.

Whenever an a is read, it triggers a clockwise rotation of the second HWP by a consistent 7°, resulting in the transformation $U_a = \begin{pmatrix} \cos 14^\circ & -\sin 14^\circ \\ \sin 14^\circ & \cos 14^\circ \end{pmatrix}$. Following the accumulation of n occurrences of a, the resulting matrix evolves into the unary operator $\begin{pmatrix} \cos n14^\circ & -\sin n14^\circ \\ \sin n14^\circ & \cos n14^\circ \end{pmatrix}$. Upon encountering one b, a counterclockwise rotation of the first HWP in U_b is initiated, where $U_b = \begin{pmatrix} \cos 14^\circ & \sin 14^\circ \\ -\sin 14^\circ & \cos 14^\circ \end{pmatrix}$. After reading m instances of b, the evolution leads to the unitary operator $\begin{pmatrix} \cos m14^\circ & \sin m14^\circ \\ -\sin m14^\circ & \cos m14^\circ \end{pmatrix}$. At the measurement part, initially, the HWP is aligned at 0° to measure the state $|H\rangle$. Subsequently, with an adjustment to 45°, the polarization shifts from H to V, enabling the assessment of the state $|V\rangle$. Consequently, the sequence involves the measurement of the $|H\rangle$ state followed by the measurement of the $|V\rangle$ state. This sequential measurement allows for the computation of the probability associated with the state $|H\rangle$.

7.2.2 Running a few experiments

We report in Table 7.2 the running of a few experiments with our optical implementation of the MO-1QFA automaton in Example 17. Values represent the probability associated with strings calculated from the experiments running the experiments within various time frames, ranging from 0.5 to 4 seconds. Note that the original MO-1QFA assigns a probability of 1 to a string of the form $\{a,b\}^*$. However, when practical considerations come into play, real-world experimental conditions introduce complexities, including noise, decoherence, and experimental imperfections. These factors can influence the implementation performance, leading to deviations from the original automaton probabilities. Achieving a probability of 1 in experimental scenarios might be challenging due to the inherent sensitivity of quantum systems to external influences. In our experiment, the observed probabilities demonstrate a remarkable level of accuracy, with values consistently exceeding 0.996 indicating successful identification of the target string.

This experiment appears successful but it suffers from the same problems as for the previous implementation. Due to our choice of a 7-degree angle when the difference in the counts of ‘a’s and ‘b’s in a string x happens to be a multiple of 90, we may incorrectly

Table 7.2 Observed probabilities in time for strings in $\{a,b\}^*$.

	0.5s	1s	1.5s	2s	2.5s	3s	4s
ε	**0.9967**	**0.9969**	**0.9964**	**0.9967**	**0.9963**	**0.9964**	**0.9967**
a	0.9342	0.9372	0.9365	0.9356	0.9387	0.9371	0.9384
b	0.9498	0.9476	0.9466	0.9491	0.9482	0.9485	0.9481
aa	0.7695	0.7676	0.7657	0.7682	0.7710	0.7725	0.7708
ab	**0.9983**	**0.9984**	**0.9988**	**0.9982**	**0.9986**	**0.9985**	**0.9983**
ba	**0.9988**	**0.9984**	**0.9986**	**0.9985**	**0.9985**	**0.9983**	**0.9983**
bb	0.8121	0.8060	0.8076	0.8107	0.8081	0.8073	0.8086
aaa	0.525	0.5272	0.5229	0.5204	0.5225	0.5189	0.5204
aab	0.9418	0.9391	0.9732	0.9366	0.9389	0.9366	0.9381
aba	0.9389	0.9391	0.9408	0.9390	0.9386	0.9371	0.9391
abb	0.9480	0.9477	0.9479	0.9478	0.9482	0.9468	0.9482
bbb	0.6140	0.6184	0.6164	0.6161	0.6184	0.6160	0.6170
aaaa	0.2702	0.2698	0.2696	0.2740	0.2731	0.2750	0.2726
aaab	0.7644	0.7652	0.7631	0.7645	0.7661	0.7683	0.7660
aabb	**0.9983**	**0.9983**	**0.9982**	**0.9984**	**0.9985**	**0.9985**	**0.9983**
abbb	0.8157	0.8085	0.8109	0.8124	0.8127	0.8109	0.8132

conclude that x belongs to the language. This implies that relying solely on this angle does not confirm identifying only the string of the language. At the current technological level, achieving rotations by an irrational multiple of π is challenging. This restriction signifies that we are currently unable to achieve theoretical precision in our experiments.

7.3 Summary

We presented the implementation of two MO-1QFAs in linear optics. The first one, although admittedly simple gives a pattern for recognizing a number of a specific consecutive symbol within a string, while the second implementation focuses on distinguishing the well-known language of balanced parentheses. Theoretically, the use of irrational numbers can provide precise and comprehensive representations, allowing for highly accurate distinctions between different patterns. However, in practical applications, the implementation of irrational numbers poses challenges.

The experiments presented here are only based on two MO-1QFA, but we believe other automata can be implemented similarly. However, implementing more complex quantum automata, such as MM-1QFAs, is still an open question.